SIMULATION OF A CARDIAC CELL. Part II: APPLICATIONS

Rossany Roche[1], Rosalba Lamanna[1], Marisol Delgado[1], François Rocaries[2],
Yskandar Hamam[2], Françoise Pecker[3]

[1]Universidad Simón Bolívar, Departamento de Procesos y Sistemas, Apartado 89000,
Valle de Sartenejas, Edo. Miranda 9995, Venezuela.
[2]Groupe ESIEE, Laboratoire Algorithmique et Architecture des Systèmes Informatiques (A2SI),
Cité Descartes, BP 99 93162, Noisy-Le-Grand, Paris, France.
[3]Institut National de la Santé et de la Recherche Médicale (INSERM), U581, Créteil, F-94010 France.

Recibido: octubre de 2008 Recibido en forma final revisado: febrero de 2009

ABSTRACT

A simulator of the cardiac cell (E-C coupling process) is developed in this work, which solves the electro-chemical model of the cell proposed by Roche *et al*. (2004). It also contains other mathematical models as well, namely, those by Tang & Othmer (1994) and Fox *et al*. (2001), for comparison purposes. The simulator allows the modification of the model parameters in correspondence with the different cellular elements, to emulate cells of different species or cells under different conditions. The paper also contains an application of the simulator for testing the sensitivity of the E-C process to drugs and inhibitors, showing its intended use as a research tool in experiment design and cardiac pathology treatment.

Keywords: Cardiac simulation, Cardiac cell, E-C coupling, Calcium dynamics, Cellular simulation.

SIMULACIÓN DE LA CÉLULA CARDIACA. PARTE II: APLICACIONES

RESUMEN

En este trabajo se presenta una ayuda computarizada para la simulación de la célula cardiaca que reproduce el comportamiento de contracción-relajación, resolviendo un modelo electro-químico de las células del músculo miocárdico desarrollado por Roche *et al*. (2004). El simulador también contiene otros modelos matemáticos como el de Tang & Othmer (1994) y Fox *et al*. (2001), a efectos comparativos. El simulador permite modificar con facilidad los parámetros del modelo asociados con los diferentes elementos celulares, para emular células de diferentes especies o bien células en diferentes condiciones. Se presenta también una aplicación del simulador para probar la sensibilidad del proceso de contracción-relajación ante diferentes drogas, demostrando cómo esta herramienta constituye una interesante ayuda en el diseño de experimentos o en la investigación sobre tratamientos de patologías cardiacas.

Palabras clave: Simulación cardiaca, Célula cardiaca, Excitación-contracción, Dinámica de calcio, Simulación celular.

INTRODUCTION

In order to develop appropriate strategies for pharmacological therapy in heart diseases, the mechanisms underlying to E-C coupling process must be well understood. A large number of "in vitro" and "in vivo" experiments, mostly qualitatively focused, are routinely carried out in biological research to study the role of several sub-cellular elements. As an alternative, a computer simulator of the cell is an excellent tool to get better understanding of the E-C coupling process and allows the substitution of an important part of laboratory experiments. It can be used to design experimental protocols or test new ones, to reduce experimental variations, to design alternative experiments and to discard "a priori" non-desirable drug effects.

Cardiac models have often been focused on only one of the chemical or the electrical aspects, in spite of the evident relationship of the two phenomena. Among the electrical models, models based on the works of Luo & Rudy (1994), Fox *et al*. (2001) and Noble (2002) can be found. They contain a complete description of the electrophysiological aspects of the cell along with some empirical blocks, and the results have been validated using patch clamp techniques.

Among the chemical models, complete descriptions of the chemical activities of the cellular elements are presented by Tang & Othmer (1994), Hamam *et al*. (2000) and Rocaries *et al*. (2004), however these models do not provide a prediction of the membrane potential and its interdependence with the calcium homeostasis.

The cell simulator presented in this paper contains a model with the complete description of the myocyte, both chemical and electrical (Roche *et al*. 2004). It is based on a "hybrid" formulation (phenomenological descriptions including some empirical elements to be identified) that ensures a certain compromise between precision and complexity of the model, and also helps to adapt it to different conditions.

In the following sections a description of the simulator of the cardiac cell is presented after a short summary of the electro-chemical model. Some simulations are shown to illustrate the process and results of a sensitivity analysis carried out on the model with the aide of the simulator. Finally, a study of the effects of some drugs on the cell behaviour is presented as examples of interesting possible applications of the simulator.

THE MODEL

In the model by Roche *et al*. (2004), the cardiac cell is represented as a system of two interconnected micro-chemical-reactors, namely the cytosol (or main reactor) and the sarcoplasmic reticulum. The different transfer processes take place between these two sub-systems, and between them and the external medium, by means of different valves (L-channels and R-channels) and pumps (SERCA, sarcolemma pump and Na^+-Ca^{2+} exchanger). They are modeled using the principles of mass transfer, fluid-dynamics and the chemical kinetics of the reactions taking place in the system. In addition, the main reactor wall is electrically charged and its potential V also modulates many of the chemical reactions involved. The detailed description of the model equations can be found in the previous companion paper (Part I) by Roche *et al*. (2009).

The equations for the main current and mass balances allow the description of three output variables of the system: Ca_i^{2+}, Ca_{SR}^{2+} and V, namely:

$$\frac{dV}{dt} = -\frac{1}{C}\left[\begin{array}{l} I_{Na} + I_{Nab} + I_{Kr} + I_{Ks} + I_{K1} + I_{to} + \\ I_{Kp} + I_{Ca} + I_{CaK} + I_{Cab} + I_{NaK} + \\ I_{NaCa} + I_{pCa} + I_{stim} \end{array}\right] \quad (1)$$

$$\frac{dCa_{SR}^{2+}}{dt} = \left(\begin{array}{l} -D_{Ca^{2+}} \cdot x_2 \cdot \dfrac{Ca_{SR}^{2+} - Ca_i^{2+}}{l} \cdot \dfrac{A_{transf}}{V_{cyt}} + \\ \dfrac{p_1 \cdot \left(Ca_i^{2+}\right)^2}{p_2^2 + \left(Ca_i^{2+}\right)^2} \end{array}\right) \cdot \frac{V_{cyt}}{V_{SR}} \quad (2)$$

$$\begin{aligned} &\frac{dCa_i^{2+}}{dt} = \\ &D_{Ca^{2+}} \cdot d \cdot \frac{Ca_0^{2+} - Ca_i^{2+}}{l} \cdot \frac{A_{transf}}{V_{cyt}} + \\ &D_{Ca^{2+}} \cdot x_2 \cdot \frac{Ca_{SR}^{2+} - Ca_i^{2+}}{l} \cdot \frac{A_{transf}}{V_{cyt}} - \\ &K \cdot \frac{1}{1 + \exp\left(\dfrac{-V}{V\max}\right)} \cdot \frac{\left(Ca_i^{2+}\right)^n}{\left(K_m^n + \left(Ca_i^{2+}\right)^n\right)} - \\ &\frac{p_1 \cdot \left(Ca_i^{2+}\right)^2}{p_2^2 + \left(Ca_i^{2+}\right)^2} - \frac{q_1 \cdot \left(Ca_i^{2+}\right)^2}{q_2^2 + \left(Ca_i^{2+}\right)^2} + \\ &k_{d2} \cdot CaM + l_{-1} \cdot x_2 \cdot R_T + l_{-1} \cdot x_3 \cdot R_T + \\ &l_{-2} \cdot (1 - x_1 - x_2 - x_3) \cdot R_T + l_{-2} \cdot x_3 \cdot R_T - \\ &k_{d1} \cdot Ca_i^{2+} \cdot M - l_1 \cdot x_1 \cdot Ca_i^{2+} \cdot R_T - \\ &l_2 \cdot x_2 \cdot Ca_i^{2+} \cdot R_T - l_2 \cdot x_1 \cdot Ca_i^{2+} \cdot R_T - \\ &- l_1 \cdot (1 - x_1 - x_2 - x_3) \cdot Ca_i^{2+} \cdot R_T \end{aligned} \quad (3)$$

The total formulation contains eighteen non-linear first order differential equations, since the integration of fifteen additional state-variables, namely d, x_1, x_2, x_3, M, CaM, m, h, j, $K_{X_{to}}$, $K_{Y_{to}}$, $K_{X_{Kr}}$, $K_{X_{Ks}}$, f, and f_{Ca} is needed to solve the model.

A fine tuning of the parameters of the model allows a good emulation of the behaviour of cardiac muscle cells from different species (rabbit, chicken, dog, human), and a better prediction when comparing the results with those from other models. These results have been reported in Roche *et al*. (2004, 2009) based on the dynamics of the output variables (Ca_i^{2+} and V). Specifically, on:

- *Curb shapes*: cyclic, with a plateau phase for V, and bell-shaped for Ca_i^{2+}.

- *Time periods*: oscillation period for $V(t_{voltage})$ in the range 200-400 ms and oscillation period for Ca_i^{2+}, ($t_{calcium}$) in

the range 800-1000 ms.

- *Maximum calcium gradient* $\Delta_{calcium}$: oscillating between 0.8 and 1.1 μM.

SIMULATION

A software tool for the resolution of the model just presented has been developed with the aide of *MatLab*® and *Simulink*®, which also includes the models by Tang & Othmer (1994) and Fox (2001).

The simulator interface main screen features a main menu, the simulator and the graphics builder (Figure 1). It contains two commands. The View command provides the functional scheme of each model. The Help command offers information on the simulator functions and parameter settings.

Simulation (Figure 1)

▪ Model selection
The user selects the model to be simulated among the three boxes that contain the parameters of each model: Kinetic model by Tang & Othmer (1994), Electric model by Fox *et al*. (2001), or Electro-Chemical model by Roche *et al*. (2004). Selection of a model box opens the simulation secondary screen, showing the parameters of the particular model, where the simulation is to be carried out (Figure 2).

• Results
Simulation results will appear (when available) on the first list on the main screen corresponding to the model indicated by the activated selection button. It is also possible to import data contained in Excel® or in .EXE files, arranged in a unique data vector (corresponding to a unique variable), to allow real data from experimental work to be charged on the second list of this screen (Figure 3).

Graphic builder (Figure 3)

Selection of the variables to be plotted on the Y axis (not more than three) and the variable on the X axis (not more than one) is made with a mouse click. The zoom capabilities of the graphics builder are activated selecting an area to detail with the right mouse button. The *Draw* button, (re)draws the graph for the selected X and Y values.

Main menu:

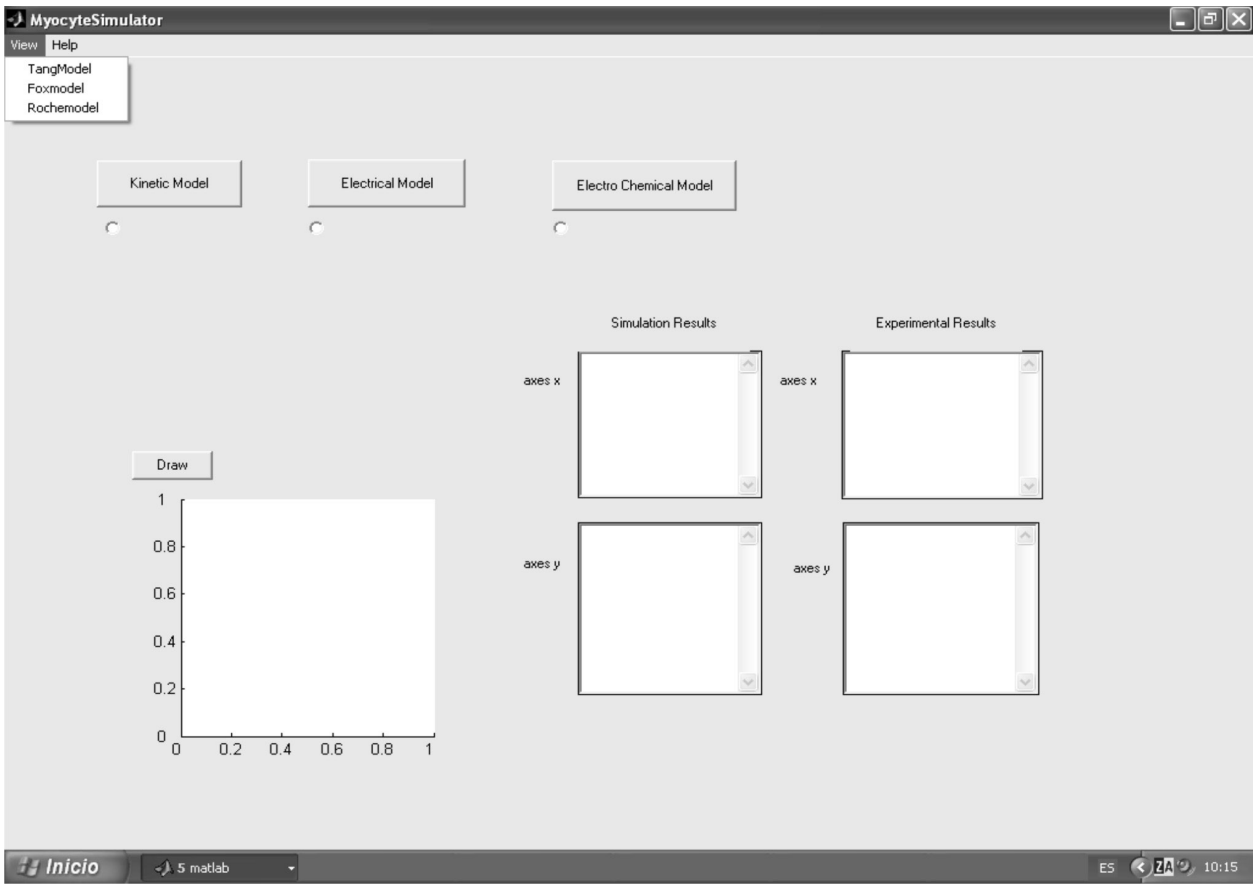

Figure 1. Simulator main screen.

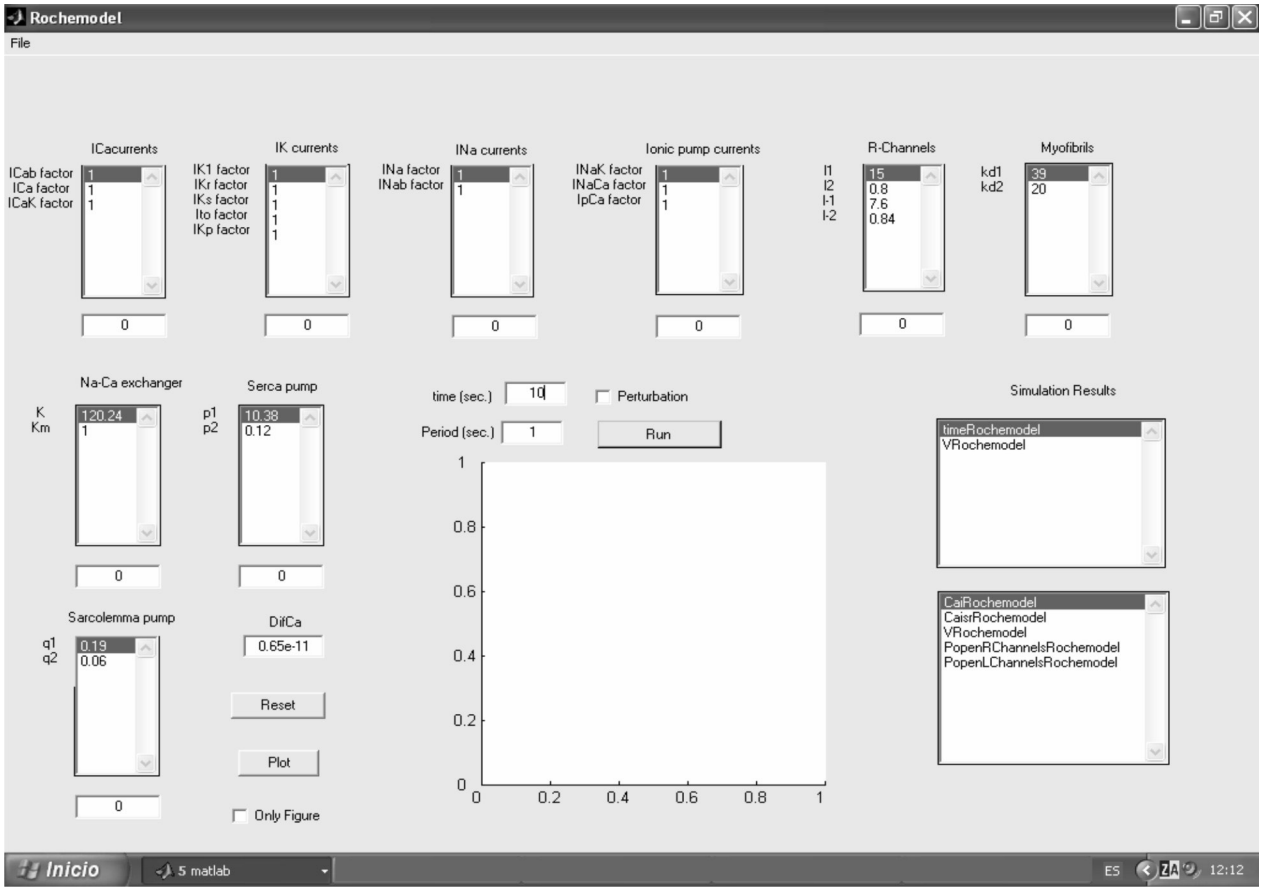

Figure 2. Simulation secondary screen for the electro-chemical model.

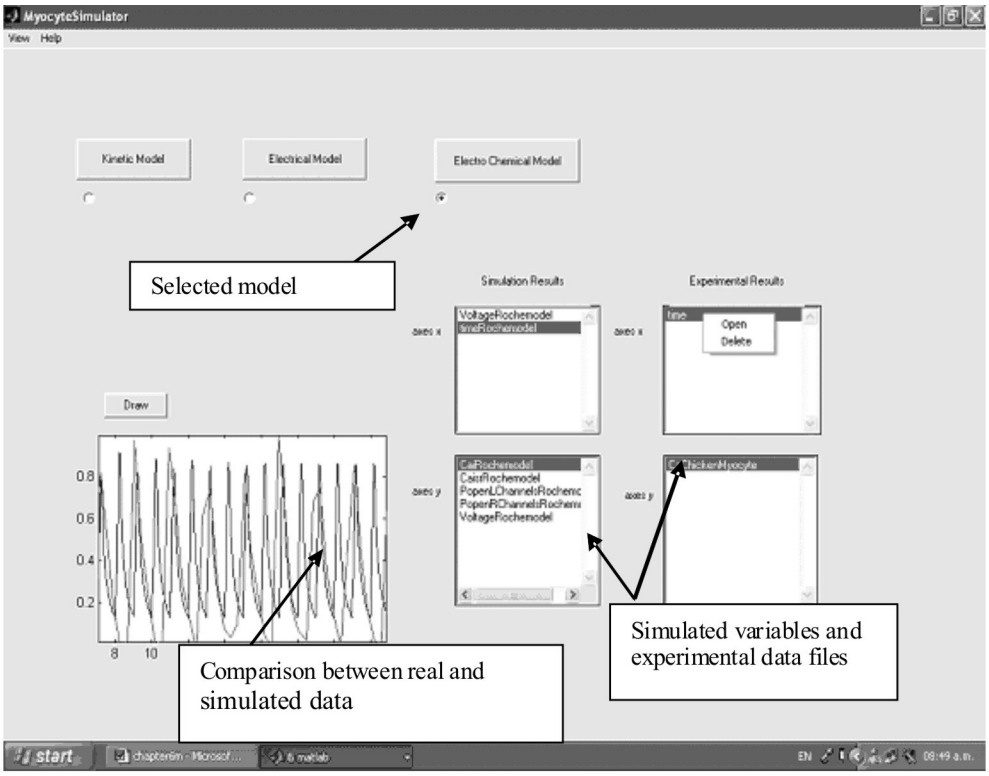

Figure 3. Simulation results on main screen.

The simulator secondary screens (one associated with each model) allow the modification of the model parameters, the actual realization of the simulation and visualization of the results (Figure 2 for the electro-chemical model).

• Model parameters

It's possible to modify a selected parameter by typing its new value in the box at the bottom of the list. The *File* menu is available to allow:

- *Save*: to memorize the corresponding parameter values. This command saves in an .MAT file the selected values of the model parameters. The user provides a name to correctly identify the set of modified parameters.
- *Open*: to use a pre-existing set of modified parameters contained in a .MAT file.
- *Exit*: to close the screen.

It is also possible to restore the initial values of the model coefficients using the *Reset* button (Figure 4).

• Simulation:

- *Simulation time*: to be fixed by the user in the "time (sec)" box (Figure 4).
- *Running*: The *Run* button initiates the simulation process. The equations of the model are integrated with *Simulink*® of *Matlab*® (v6.5), using a variable-step numerical solver based on the algorithm by Klopfenstein (1971). This method is relatively fast and accurate, and allows the modification of the relative error tolerance and absolute error tolerance values (Shampine & Reichelt, 1997). During the simulation process the *Run* button appears as *Processing*.
- *Model Perturbations*: The activation of the *Perturbation* option allows the realization of simulations with modified parameters, to test the model. An active button designated by *Set 1* appears (Figure 5) to let the user charge an initial set of parameters, and changes afterwards to *Set 2* to accept the modified or "perturbed" parameters. The simulation is carried out with the initial coefficients for the first half of the total simulation time, and then switching to the changed or perturbed parameters.
- *Results*: Once the simulation concludes, the set of simulated variables is deployed in the abscissas and ordinate of the graphic builder, with easily identifiable names (Figure 4). Selecting each variable with the right mouse button makes available the *Save* option. The *Save* command creates an .EXE or .MAT file containing the selected variable with the name assigned by the user.

• Graphics builder

The variables to be plotted are picked up with a mouse click. The zoom capabilities of the graphics builder are activated selecting an area to detail with the right button of the mouse. It is also possible to see the graph in a separated window, by clicking the *Graphic* button. The *Erase* button eliminates a previously drawn graph. The *Draw* button,

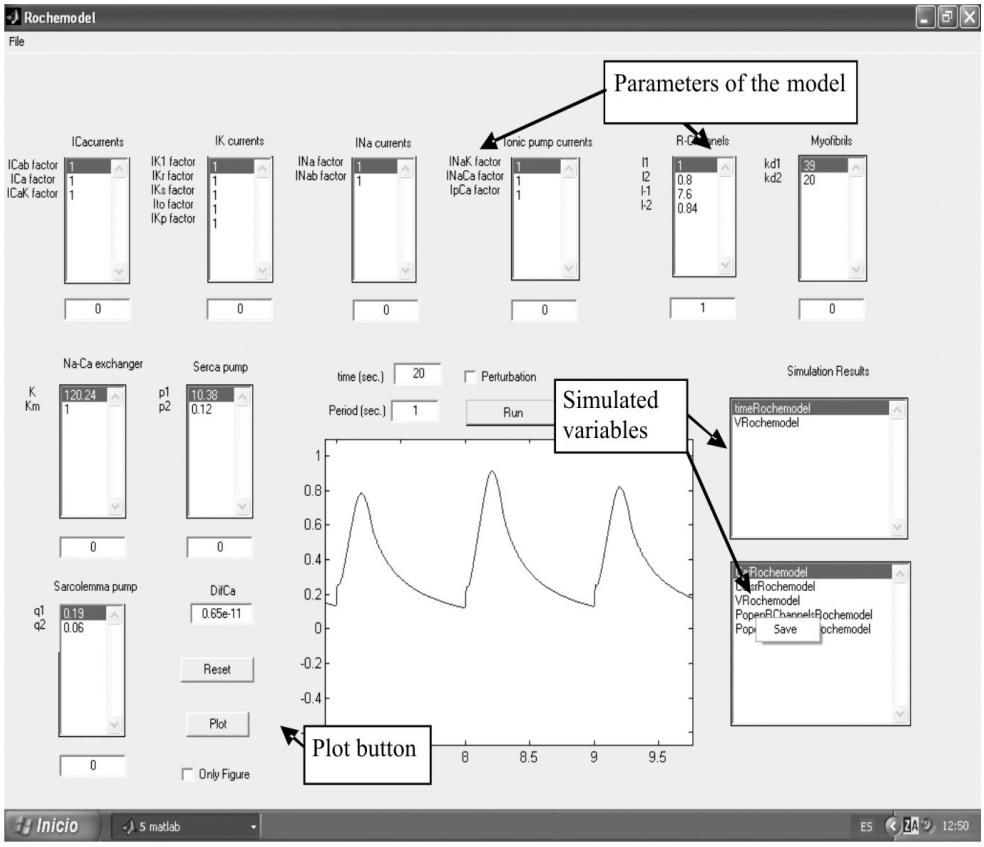

Figure 4. Simulation screen for the electro-chemical model.

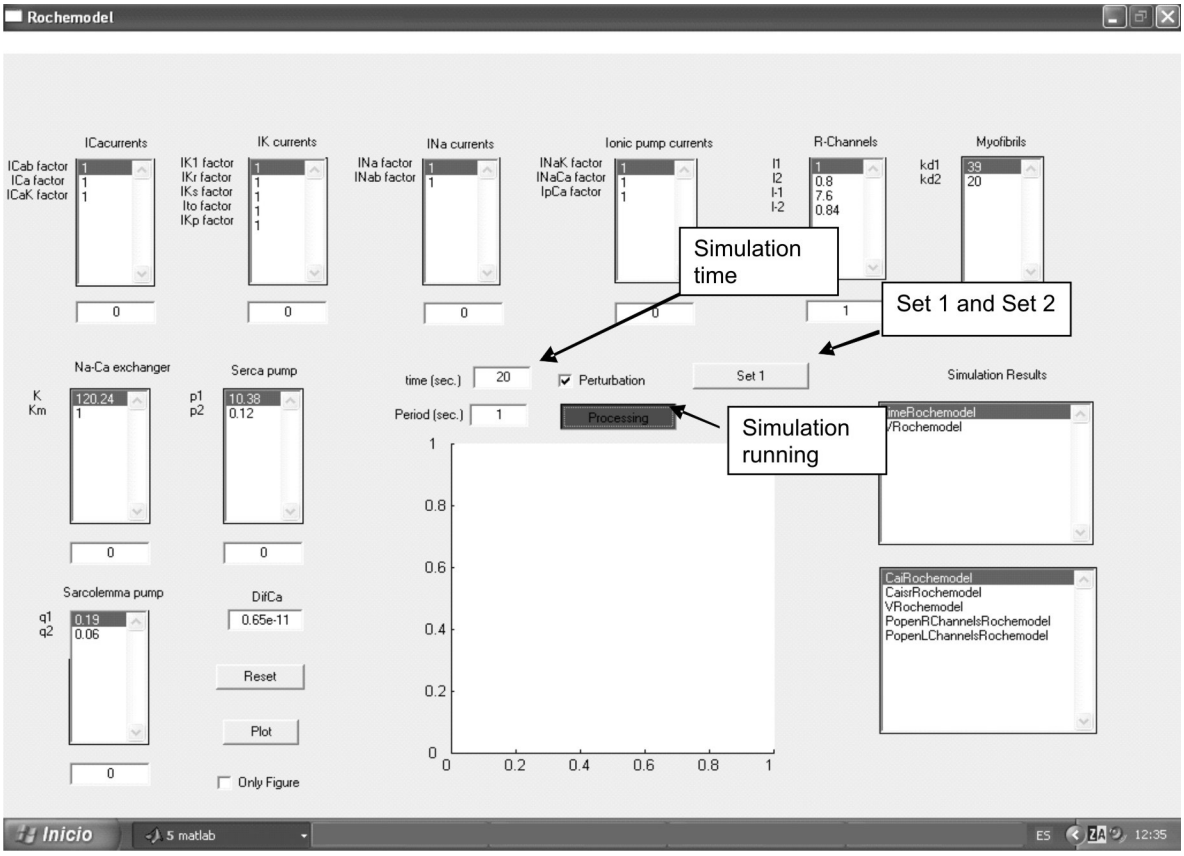

Figure 5. Simulating with parameter perturbations.

(re)draws the graph for the selected variables.

SIMULATOR APPLICATION: SENSITIVITY ANALYSIS OF THE MODEL

A good number of calcium and voltage time responses were obtained with the aide of the simulator, and the parameters adjusted to emulate real experimental data. The flexibility of the simulator, that deploys all the important parameters of each cell element, easily allows the parameter modifications.

An important result of the extensive validation procedures carried out with the simulator, is precisely an expert knowledge of the effects of different coefficient alterations in specific model components on the shape and duration of the cell time responses. The methodical testing of these effects, namely the sensibility analysis of the model, includes two steps:

1) The simulation of the model with the standard parameters for a generalized mammal cardiac cell, up to steady-state (40 s. of simulation time).

2) The "perturbation" of the model, meaning the simulation with an altered element (one parameter at a time), being a "stimulation" of the element if the parameter is increased, or an "inhibition" if it is decreased.

The following results from the sensibility analysis can be reported:

- Some elements do not have any significant effect on the dynamics and therefore can be simplified or eliminated from the model, as in the case of perturbations of q_1 parameters and $\bar{I}_{pCa\max}$ associated with the chemical and electrical activity of the sarcolemma pump (Figures 6 and 7).

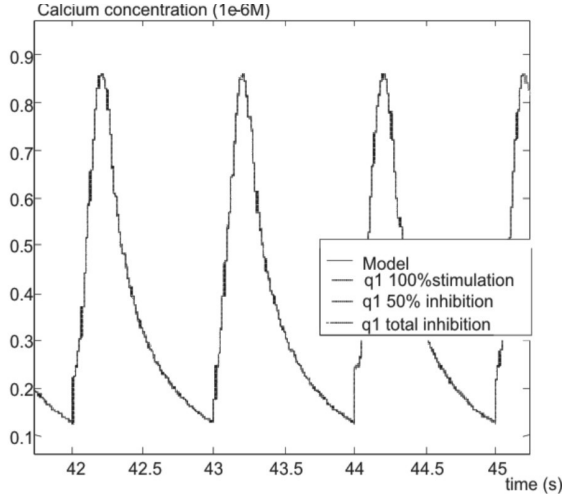

Figure 6. Effects on Ca_i^{2+} of parameter q_1.

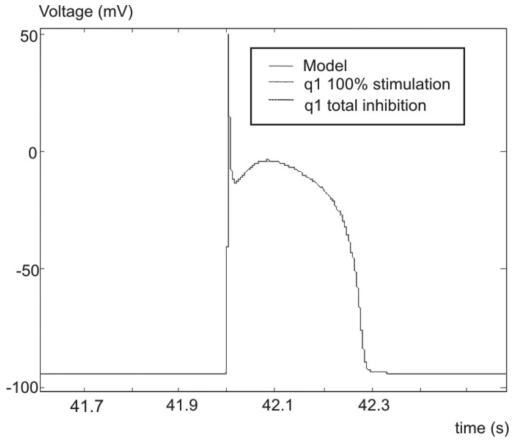

Figure 7. Effects V on of perturbation in parameter q_1.

- The model is very sensitive to some elements which description is therefore a key issue, as in the case of the Na+-K+ pump. In Figures 8 and 9 some results of parameter perturbations in this element show important alterations in the process outputs.

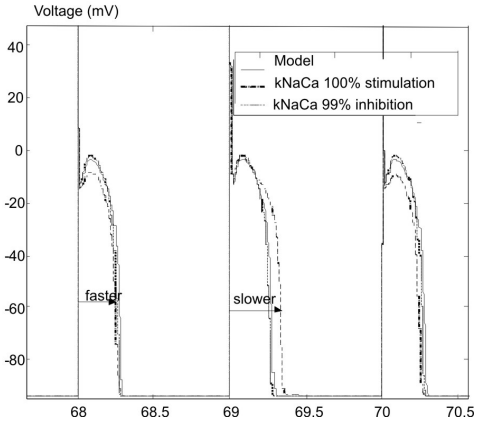

Figure 8. Effects on V dynamics of parameter $\boldsymbol{k}_{NaCa}$.

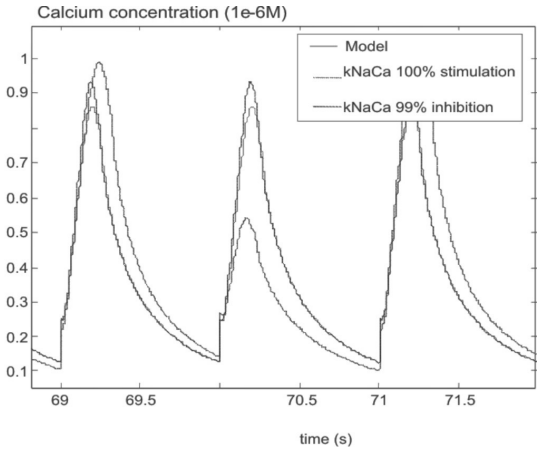

Figure 9. Effects on Ca_i^{2+} of parameter k_{NaCa}.

- The emulation of abnormal behaviors (pathologies) of the cell along with the identification of the cellular elements that cause them can be achieved with the sensitivity analysis of the model. As an example, the inhibition of parameter K_{d1}, which is related to the myofibrils kinetics, emulates a typical situation of cardiac insufficiency, this is the decrease in chemical affinity between the myofibrils and the calcium ions and therefore the loss of contractile power of the cell (Figures 10 and 11). Another example can the seen in Figure 12, where the altered outputs obtained by changes in the chemical and electrical activities of the L-channels, through parameters F_d and P_{Ca}, correspond to cardiac arrhythmias.

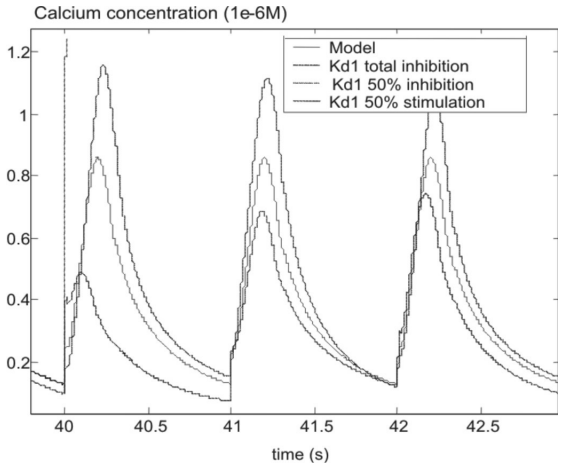

Figure 10. Effects on Ca_i^{2+} dynamics of parameter K_{d1}.

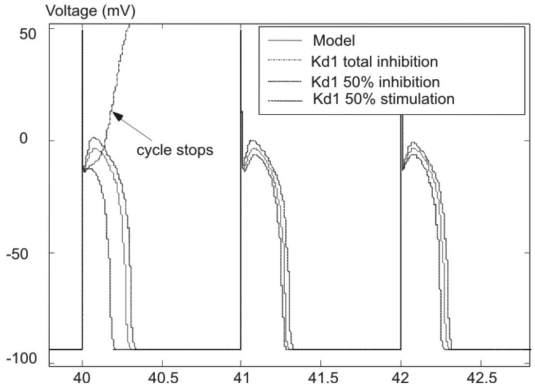

Figure 11. Effects on V dynamics of parameter K_{d1}.

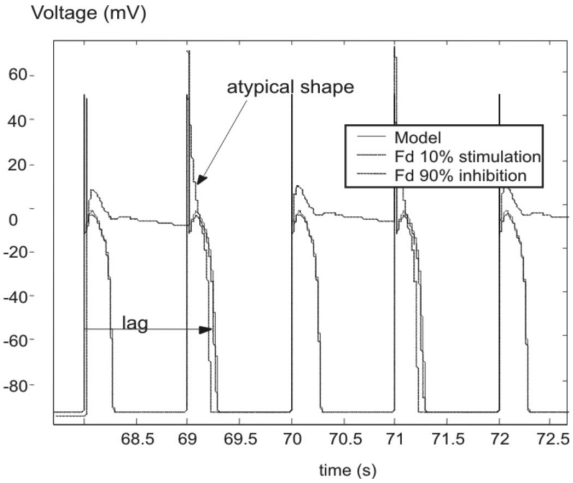

Figure 12. Effects on V dynamics of parameter F_d.

Even if several kind of parametric alterations can produce similar effects, the results of this sensitivity analysis allow the identification of the cellular elements and therefore which parameters must be altered to produce changes on each phase of the calcium or the voltage dynamics. This information is summarized in Figures 13 and 14.

It is easy to foresee at this point the applications of the simulator to support pharmacological research for instance, because it can be used to study the effects of different drugs by determining which alterations in cellular elements are induced by them.

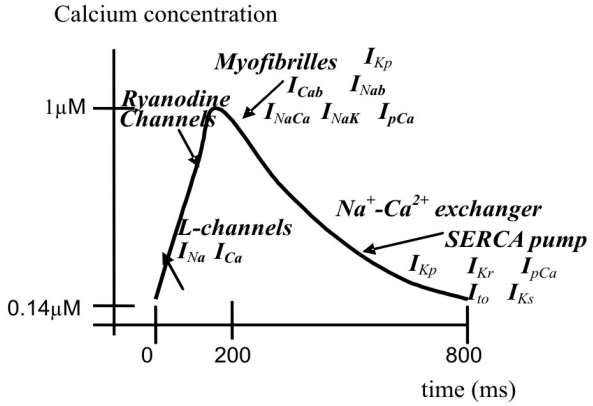

Figure 13. Parameter sensitivity on the calcium dynamics.

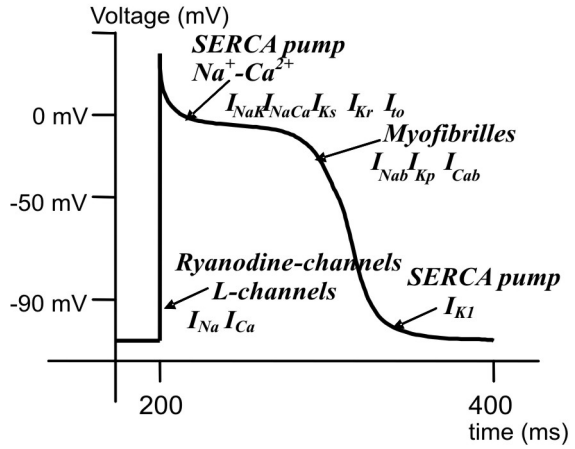

Figure 14. Parameter sensitivity on the membrane potential dynamics.

SIMULATOR APPLICATION: TESTING OF DRUGS EFFECTS

Previous works (Tang & Othmer, 1994; Hamam *et al*. 2000; Luo & Rudy, 1994; *Fox et al*. 2001) cannot explain myocyte behavior in presence of some specific substances because the models only take into account the electrical or the chemical aspects of the cell. Results of testing the effects of several drugs using the electro-chemical model are presented in this section. Reproduction of the altered behavior of the myocyte under drug injection is achieved with the aide of the simulator to methodically modify the parameters of the model, identifying specifically the cellular elements affected by each drug. This may help to clarify several questions about the abnormal E-C coupling process and to explore alternative therapies for cardiac diseases.

Experimental data for chicken myocytes under the injection of *Caffeine*, *Forskolin*, *Ruthenium red* and *Thapsigargin* drugs have been provided by *INSERM*, following experimental protocols similar to those used by (Rocaries *et al*. 2004).

A study for each drug effect separately has been carried out according to the following methodology:

- The set of parameters corresponding to the drug effect are identified by taking into account the sensitivity study of the model presented in the previous section, and reported knowledge found in bibliographical reviews.

- By trial and error method, the selected set of parameters are modified in order to reproduce the altered myocyte behaviour.

- The simulation results are compared with the experimental results. The protocol for this comparison is to obtain the normal behavior in the first place and then, after of 40 minutes of simulation, to alter the parameters set (using the "Perturbation" button in the simulator secondary screen, Figure 5). This protocol also corresponds to the experimental drug injection.

Caffeine effects

Caffeine is used in muscle research to study the role of the sarcoplasmic reticulum in the E-C coupling process (Smith & Steele, 1998). *Caffeine* binds to a specific site on the R-channels inducing a Ca^{2+}-independent activation of the channels, with increases in both the frequency and duration of the channels openings (Duke & Steele, 1998). It is also reported by Smith & Steele (1998), that *Caffeine* may lower the Ca^{2+} within the SR, to a sufficient level to stimulate the SERCA pump by a mechanism that is not yet clear. Bassani *et al*. (1998), applying rapid injections of 10mM-Caffeine observed a rate of the SERCA pump of about 3-4 times faster than that of the Na^+-Ca^{2+}-exchanger.

Experimental data provided by *INSERM* is obtained injecting a pulse of 10 mM-*Caffeine*, 40 minutes after the normal behavior of the chicken myocyte is reached. Results of this experiment show that calcium concentration values in the cytosol are increased, however the concentration gradient is slightly reduced (Δ_{calcio} = 0,9 μM whereas Δ_{calcio} =1 μM under normal conditions) indicating that probably the SERCA pump activity is stimulated such as observed by Bassani *et al.* (1998) and Smith & Steele (1998). Reduction of calcium gradient in the cytosol using *Caffeine* injection is also observed by Zhang *et al. (*1999). In order to reproduce the facts previously mentioned three parameters of the model have been altered: increasing of l_1 in order to increase the open probability of R-channels, stimulus of p_1 (SERCA

pump) and inhibition of Na^{+}-Ca^{2+}-exchanger activity (rate reduction of *K*).

The set of values of the best fit parameters are shown in the Table 1. Figure 15 and 16 present the comparison between experimental data and simulations results for calcium concentration. The model reproduces the *Caffeine* effects in the chicken myocyte, that is, calcium concentration value increased in the cytosol and calcium gradient decreased.

Table 1. Modified values of parameters set for drug effects.

Drug	Effect	Parameter	Modified Value /Original Value
Caffeine	Stimulus	l_1 ($\mu M^{-1}s^{-1}$)	22.5 /(15)
	Stimulus	p_1 (μMs^{-1})	103.8 / (10.38)
	Inhibition	K (μMs^{-1})	60.12 / (120.24)
Forskorlin	Inhibition	K(μMs^{-1})	36.072 / (120.24)
	Inhibition	I_{NaK}	0.7/(1)
Ruthenium red	Inhibition	l_1 ($\mu M^{-1}s^{-1}$)	10.5 /(15)
	Stimulus	p_1 (μMs^{-1})	30.38 / (10.38)
	Inhibition	I_{Ca}	0.9/ (1)
	Inhibition	K (μMs^{-1})	4.8096 / (120.24)
Thapsigargin	Inhibition	l_1($\mu M^{-1}s^{-1}$)	7.05 /(15)
	Inhibition	p_1(μMs^{-1})	3.1140 / (10.38)
	Inhibition	K(μMs^{-1})	30.06/ 120.24)
	Stimulus	I_{NaCa}	2 / (1)
	Stimulus	I_{Cab}	1.3 / (1)

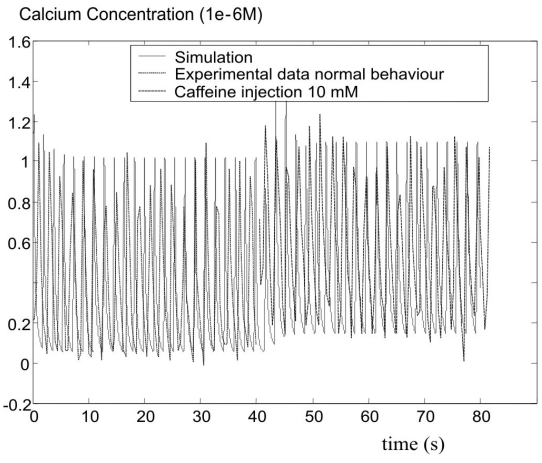

Figure 15. Experimental and simulated data for *Caffeine* effect on calcium concentration in the cytosol.

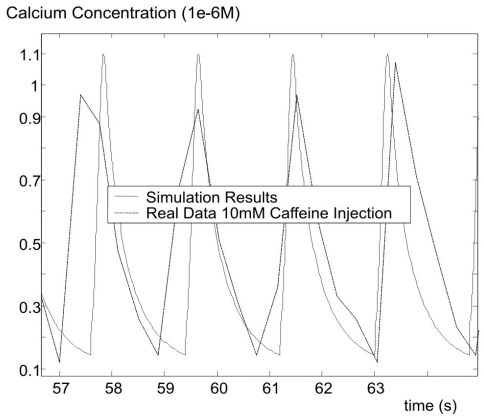

Figure 16. Experimental and simulated data for *Caffeine* effect in calcium concentration in the cytosol (detail).

Additionally, in Figure 17 the increasing of open R-channels, from range of probability 0,1 - 0,5 to range 0,2 - 0,55 can be noticed, agreeing with SITSAPESAN (1998) and with Duke & Steele (1998). On other hand, Figure 18 shows that the results for SERCA pump and Na^{+}-Ca^{2+} exchanger flow-rates are similar to results found by Bassani *et al. (*1998), this is the SERCA pump rate being faster than that of the Na^{+}-Ca^{2+}-exchanger.

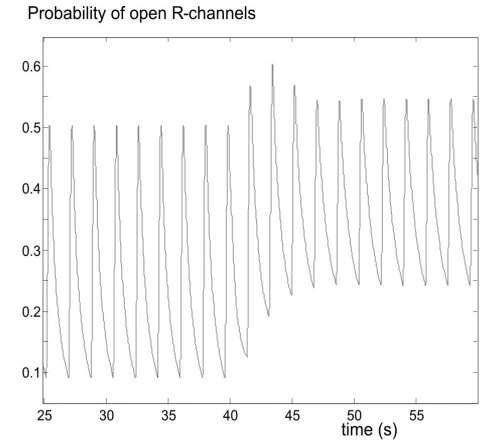

Figure 17. Simulated probability of open R-channels (variable x_2) for Caffeine effect.

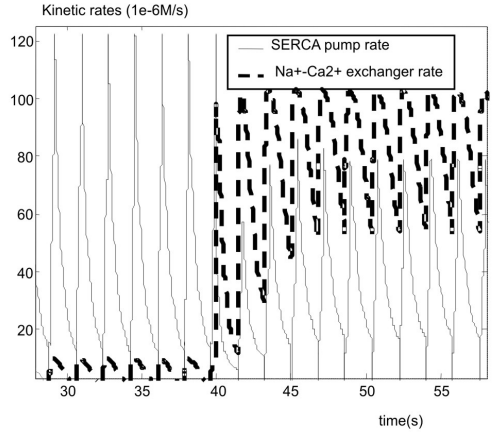

Figure 18. Simulated SERCA-pump and Na^{+}-Ca^{2+}-exchanger rates (FQ_{SERCA}, FQ_{ENa}-$_{Ca}$) for *Caffeine* effect.

Forskolin effects

Forskolin increases the level of the cell-regulating compound called cyclic adenosine monophosphate (*cAMP*) - one of the key regulators of *ATP* cycle (Zhang & Wong, 1998). The raise of *cAMP* concentration in the heart leads to an increased force of contraction. This may be useful in congestive heart failure and various heart diseases. Furthermore, Forskolin appears to relax the smooth muscles in the walls of the arteries. The relaxation of the arteries decreases blood pressure, pain due to angina, and strain on the heart. Tominaga *et al*. (1995), studied the effects of 1μM *Forskolin* injection on guinea-pig ventricular myocytes concluding that, during current-clamp experiments, *Forskolin* reduces the action potential significantly, from 250 ms to 201 ms. Also, *Forskolin* was found responsible for increasing the magnitude of hyperpolarized currents in mouse embryo pacemaker cells (Song *et al*. 2002).

Experimental data provided by the *INSERM* shows that 30 hours after a 1 μM *Forskolin* injection the cytosol calcium cycles become very unstable (Figure 19). This strong perturbation is similarly observed in the model when the Na^+-Ca^{2+}-exchanger is perturbed. Additionally, low membrane potential and unstable calcium cycles are also produced by perturbations on the I_{NaK} current. Based on the previous sensitivity study and analysis, we have selected the K parameter of the Na^+-Ca^{2+} exchanger and the coefficient $I_{NaK}{}_{max}$ of the I_{NaK} current as the parameters linked to the Forskolin effects. After few trials, the appropriate parameters values are found as reported on Table 1. Simulations of the model after the modifications of just these two parameters are close to real *Forskolin* effects, as can be observed in Figure 19.

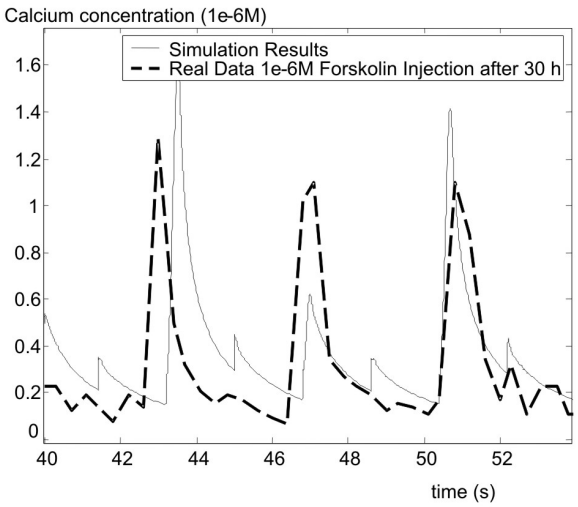

Figure 19. Experimental and simulated data for *Forskolin* effects in calcium homeostasis.

However, *Forskolin* effects on the model are observed immediately and not 30 hours later as with the experimental data. This may be associated to the *ATP* cycle dynamics which is not included in the model. In future works we suggest to add the chemical reactions of the *ATP* cycle in order to observe its impact on the *Forskolin* effects. Despite this setback, the model involving chemical and electrical aspects has proved its adaptability to test the strong *Forskolin* effects, where other models that do not include the electric dynamics fail (Rocaries *et al*. 2004). Figure 20 contains the voltage simulations results for *Forskolin* injection showing that the membrane potential is faster, agreeing with the results by Tominaga *et al*. (1995), but at the same time the voltage cycle becomes strongly unstable.

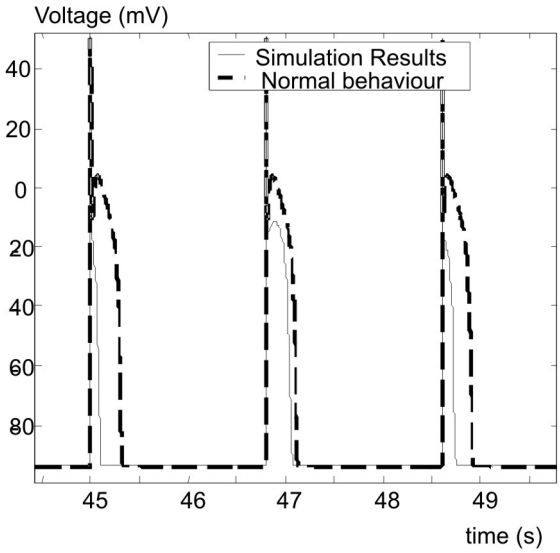

Figure 20. Voltage simulation results for *Forskolin* effects.

Ruthenium red effects

Ruthenium red is known as an inhibitor of sarcoplasmic reticulum Ca^{2+} release. Lukyanenko *et al*. (2000), report inhibitions of the probability of open R-channels (20-50% of reduction) in rat ventricular myocytes with concentrations of 0.1 μM, 1 μM and 5 μM on a *Ruthenium red* injection. Others results of this work show that *Ruthenium red* (5μM) increases the sarcoplasmic reticulum calcium concentration from 151 μM to 312 μM. *Ruthenium red* is also recognized to inhibit the mitochondrial Ca^{2+} uptake mechanism, which in turn produces a delay in the recovery of L-channels calcium currents reducing the muscle contractibility and generating ventricular tachycardia (Sánchez *et al*. 2001). Experimental Data of *INSERM* showing the effects of 1 μM *Ruthenium red* injection on calcium concentration in the cytosol can be seen in Figure 21. After 140 minutes, *Ruthenium red* perturbation changes enormously the calcium gradient. Resting calcium value is modified from 0.1 μM to 0.75 μM reducing calcium gradient significantly (~70%).

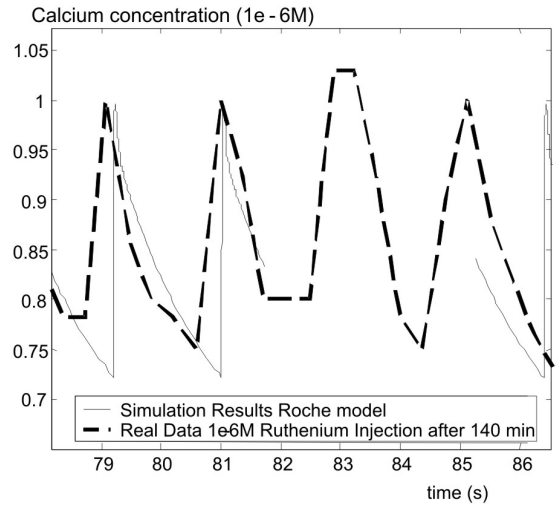

Figure 21. Experimental and simulated data for *Ruthenium red* effects in calcium homeostasis.

We have observed, during the sensitivity study of the model, that inhibition of the Na^{+}-Ca^{2+} exchanger rate produces changes in the resting calcium value in the cytosol. Based on this aspect and taking into account the works by Lukyanenko *et al*. (2000) and Sánchez *et al*. (2001), we have selected the following set of parameters to be altered in order to reproduce *Ruthenium red* effects: l_1 (reduction of open probability of R-channels), p_1 (sarcoplasmic reticulum calcium concentration increasing), I_{Ca} factor (delay of L-channels) and K (resting calcium value perturbation).

Table 1 shows the new parameters values adjusted by trial and error. Simulations of *Ruthenium red* effects (Figure 21) are instantaneous instead of delayed as the experimental results, which occur 140 minutes later. The model does not include a mitochondrial description, and this may be the cause of the delay in the experimental *Ruthenium red* effects. Despite this aspect, the simulation results fit well to the experimental data. On the other hand, in Figure 22, it can be noticed that the reduction of the fraction of open R-channels agrees with Lukyanenko *et al*. (2000). Figure 23 shows the increasing of sarcoplasmic reticulum calcium concentration by *Ruthenium red* effects. This increase is larger that the values reported by Lukyanenko *et al*. (2000), however the cellular species in both cases are different (rat vs. chicken ventricular myocyte).

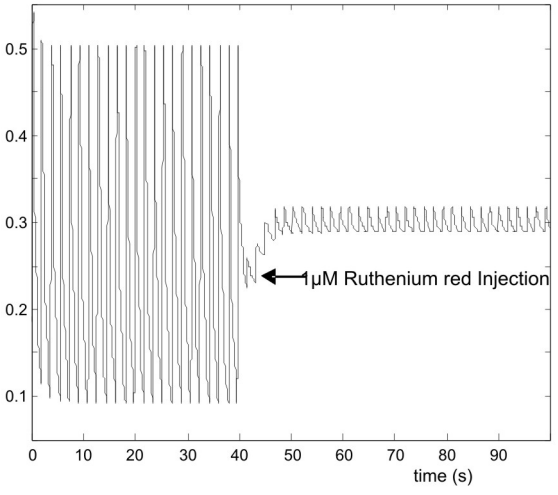

Figure 22. Probability of open R-channels for *Ruthenium red* effects.

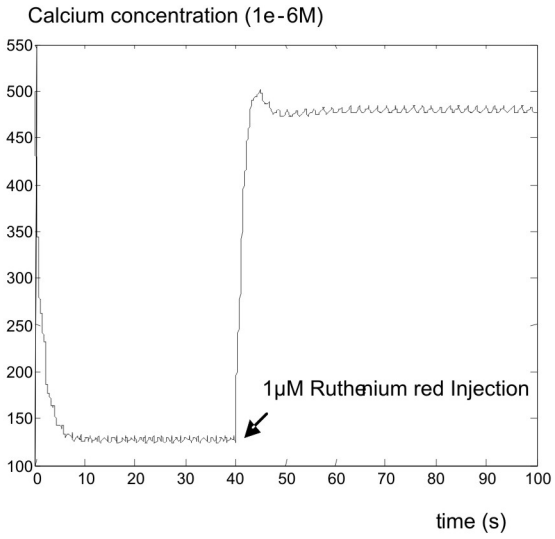

Figure 23. Calcium concentration in sarcoplasmic reticulum after *Ruthenium red* injection.

Thapsigargin effects

Thapsigargin has been used as a selective inhibitor of the SERCA pump in cardiac myocytes (Kirby *et al*. 1992). Gaugham *et al*. (1999), were able to virtually eliminate sarcoplasmic reticulum using *Thapsigargin*. In their experiment, they show that *Thapsigargin* had no effect on the action potential shape. Results of Ginsburg *et al*. (1998), show that, when the SERCA pump rate was slowed by 39% through a 0.4 μM *Thapsigargin* injection, the sarcoplasmic reticulum calcium concentration decreased by 20%. Vigne *et al*. (1992) report that *Thapsigargin* injection rapidly raises calcium concentration in the cytosol followed by a depression. Similar results are reported in the experimental data of *INSERM* (Figure 24) where calcium concentration in the cytosol is increased and rapidly decreased producing instable calcium cycles. Wu *et al*. (2001) suggest that *Thapsigargin* is also an inhibitor agent of the R-channels.

We have found that perturbations in I_{Cab} current produces an increase in calcium concentration in the cytosol followed by decrease. Also modifications of I_{NaCa} current and Na^{+}-Ca^{2+} exchanger rate have similar effects. Taking into account these aspects we have selected the following parameters set in order to test *Thapsigargin* effects on chicken myocyte: l_1 (R-channels inhibition), p_1 (SERCA pump inhibition), K, I_{NaCa} and I_{Cab} (unstable calcium cycles). Table 1 shows the values

of the parameters adjusted by trial and error. Figure 24 shows the comparison between experimental data and simulation results where it may observed that the model produces the *Thapsigargin* effects on myocyte close to experimental data.

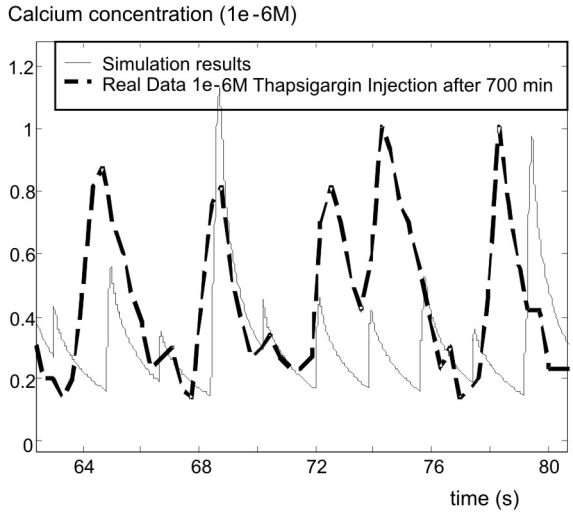

Figure 24. Experimental and simulated data for *Thapsigargin* effects in calcium homeostasis.

Simulation results of R-channels are observed in Figure 25, where the R-channels are inhibited according to the observations by Wu *et al*. (2001). The simulation results of the sarcoplasmic reticulum calcium concentration are shown in Figure 26. A decreasing in calcium concentration is observed (50% for chicken myocyte) following the same trend as in Ginsburg's report (1998) (20% for adult ferret ventricular myocytes). Voltage simulation results are presented in Figure 27, where a faster voltage cycle can be noted due to the *Thapsigargin* injection, although the alterations in shape reported by Gaughan *et al.* (1999) are not observed.

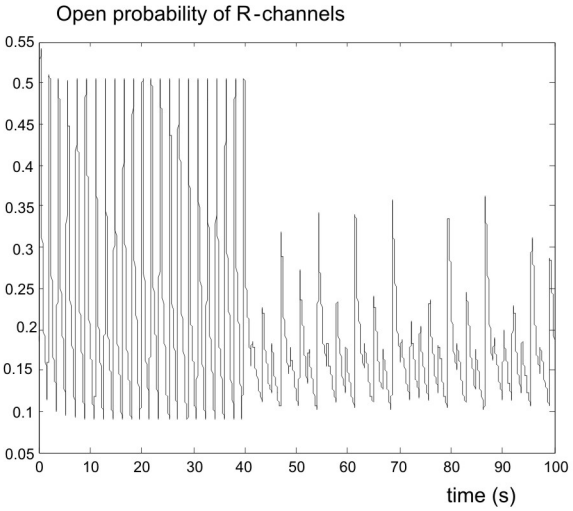

Figure 25. Simulation of probability of open R-channels after *Thapsigargin* injection.

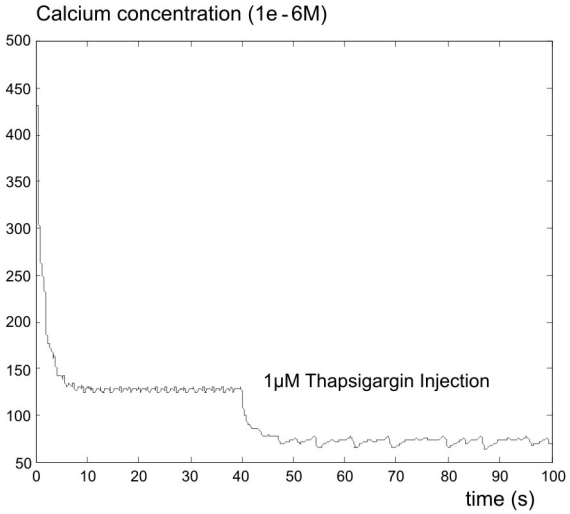

Figure 26. Sarcoplasmic calcium concentration after *Thapsigargin* injection.

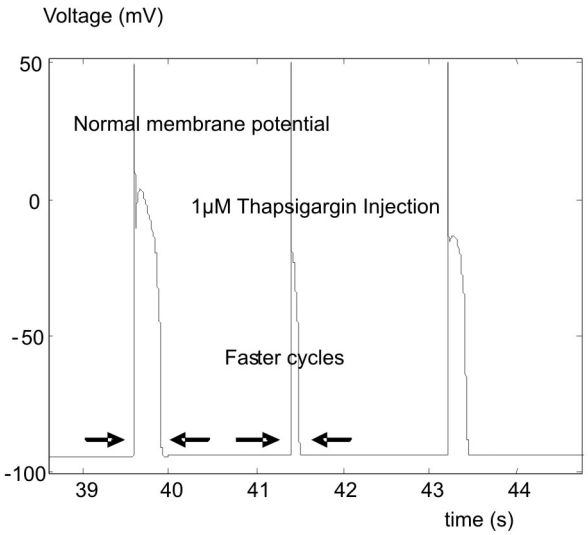

Figure 27. Voltage simulation results for *Thapsigargin* effects.

Finally, although previous works don't state any association between *Thapsigargin* effects and the Na^{+}-Ca^{2+} exchanger activity, the results by Gaughan *et al.* (1999) have established that when the SERCA pump is inhibited the Na^{+}-Ca^{2+} exchanger contributes to the E-C coupling process producing altered calcium cycles similar to those present in the experimental data of *INSERM*. Therefore to reproduce the *Thapsigargin* effects, the kinetic and the electrical parameters related to the Na^{+}-Ca^{2+} exchanger are to be altered. These results may be further improved by adding a more complete description of the kinetics for the Na^{+}-Ca^{2+} exchanger, since Gaughan *et al.* (1999) have suggested that the Na^{+}-Ca^{2+} exchanger works in an additional mode (reverse mode) which is not described by this model. This reverse mode may contribute to *Thapsigargin* delay (700 minutes), which is not reproduced at the moment by the simulator.

CONCLUSIONS

A simulator of the cardiac cell has been developed, devoted to the solution of a global electro-chemical model of the cell (Roche *et al.* 2004). It describes a cardiac cell integrating the electrical and chemical dynamical aspects of the different components in the cytosol, the sarcoplasmic reticulum, and the cellular membrane, producing the expected time responses of the excitation-contraction (E-C) coupling, i.e. the oscillatory-bell-shaped curve in calcium dynamics and the characteristic plateau phase in membrane potential.

The simulator has been used to carry out a sensibility analysis of the model, allowing to explore the coherent behaviour of each model component, to identify key elements (as the Na+K+ pump), or even elements that do not have influence on the process outputs (as the sarcolemma pump). Finally the simulator can be used to emulate abnormal situations (cardiac pathologies). This feature extents greatly its applications in order to test drug effects on the myocyte.

In the testing of drug effets, the phenomenological structure of the model allows the identification of the cellular sub-systems that are related to specific changes in the process dynamics. The parameters modifications reproduce the experimental drug effect allowing to identify the cellular mechanism altered. This aspect is an important contribution in the development of new treatments.

Some necessary improvements of the model by Roche *et al*. (2004) such as an alternative kinetic description of the Na^{+}-Ca^{2+}, or some other additions required to well adjust the model to experimental data, have also been pointed out.

ACKNOWLEDGEMENTS

The work presented in this paper is the result of the French Venezuelan collaboration research project entitled: “Modeling of the cardiac phenomena: from the cell to the organ”. The authors gratefully acknowledge the financial support of ECOS Nord (France), FONACIT, Universidad Simón Bolívar and FUNDAYACUCHO (Venezuela).

REFERENCES

Bassani, R., Bassani, J., Bers, D. (1992). Mitochondrial and sarcolemmal Ca2+ transport reduce [Ca2+] i during caffeine contractures in rabbit cardiac myocytes. Journal of Physiology. Vol. 453, Issue 1, pp. 591-608.

Berridge, M., Bootman, M., Rodeirck, H. (2003). Calcium Signaling: Dynamics, Homeostasis and Remodeling. Nature Reviews. Vol. 4; pp. 517-529.

Bray, D., Bruce, a., Lewis, J., Raff, M., Roberts, K., Watson, J. (1994). Molecular Biology of the Cell. New York Garland, United States of America, pp. 1219.

Duke, A. & Steele, D. (1998). Effects of caffeine and adenine nucleotides on Ca2+ release by the sarcoplasmic reticulum in sponin-permeabilized frog skeletal muscle fibres. Journal of Physiology. Vol. 513.1, pp. 43-53.

Fox, J., Micharg, J., Gilmour, R. (2001). Ionic mechanism of electrical alternants. Am. J. Physiol. Heart. Circ. Physiol. Vol. 282; pp. H516-H530.

Gaughan, J., Furukawa, S., Jeevanandam, V., Hefner, C., Kubo, H., Margulies, K., McGowan, B., Mattiello, J., Dipla, K., Piacentino, V., Li, S., Houser, S. (1999). Sodium/calcium exchange contributes to contraction and relaxation in failed human ventricular myocytes. American Journal of Physiology. Vol. 277, pp. H714-H724.

Ginsburg, K., Weber, C., Bers, D. (1998). Control of Maximum Sarcoplasmic Reticulum Ca Load in intact Ferret Ventricular Myocytes. Journal of General Physiology. Vol. 111, pp. 491- 504.

Hamam, Y., Pecker, F., Rocaries, F., Lorino, H., Pavoine, C., Natowicz, R. (2000). Identification and modelling of calcium dynamics in cardiac myocytes. SIMPRA Vol. 222; pp. 01-14.

Kirby, Y., Sagara, S., Gaa, G., Inesi, W., Lederer, T., Rogers, T. (1992). Thapsigargin inhibits contraction and Ca^{2+} transient in cardiac cells by specific inhibition of the sarcoplasmic reticulum Ca^{2+} pump. Journal of Biological Chemistry. Vol. 267, Issue 18, pp.12545-12551.

Klopfenstein, W. (1971). Numerical differentiation formulas for stiff systems of ordinary differential equations. RCA Review, Vol. 32; pp. 447-462.

Lecarpentier, Y., Coirault, C., Chemla, D. (1996). Régulation cellulaire et moléculaire de la contraction cardiaque. Méd. Thér., Vol. 2; pp. 113-122.

Li, G., Zhang, M., Satin, L., Baumgarten, C. (2002). Biphasic effects of cell volume on excitation-contraction coupling in rabbit ventricular myocytes. Am. J. Physiol. Heart. Circ. Physiol., Vol. 282; pp. H1270-H1277.

Lukyanenko, V., Gyorke, I., SubramaniaN, S., Smirnov, A., Wiesner, T., Gyorke, S. (2000). Inhibition of Ca2+ sparks by ruthenium red in permeabilized rat ventricular myocytes. *Biophysical* Journal. Vol. 79, pp. 1273-1284.

Luo, C. & Rudy Y. (1994). A Dynamic Model of the Cardiac Ventricular Action Potential, Part I and II. Circ. Res., Vol. 74; pp. 1071-1096 and 1097-1113.

Maclennan, D., Kranias, E. (2003). Phospholamban: A Crucial Regulator of Cardiac Contractibility. Nature Reviews. Vol. 4, pp. 566-577.

Michailova, A., Delprincipe, F., Egger, M., Niggli, E. (2002). Spatio-temporal Features of Ca^{2+} Buffering and

Diffusion in Atrial Cardiac myocytes with Inhibited Sarcoplasmic Reticulum. Biophys. J. , Vol. 83; pp. 3134-3151.

Noble, D. (2002). Modelling the heart: insights, failures and progress. BioEssays. Vol. 24; pp. 1155-1163.

Piacentino, V., Weber, C., Chen, X., Weisse-Thomas, J., Margulies K. Bers, D., Houser, S. (2003). Cellular Basis of Abnormal Calcium Transients of Failing Human Ventricular myocytes. Circ. Res., Vol. 92; pp. 651-658.

Rocaries, F., Hamam, Y., Roche, R., Lamanna, R., Delgado, M., Pecker, F., Pavoine, C., Lorino, H. H. (2004). Calcium Dynamics in Cardiac myocytes: a model for drugs effect description. SIMPRA, Vol. 12; pp. 93-104.

Roche, R., Lamanna, R., Delgado, M., Rocaries, F., Hamam, Y., Pecker, F. (2004). Calcium homeostasis and membrane potential in cardiac myocyte: an electrochemical model. Proc. 5th EUROSIM Congress on Modelling and Simulation. Editors: Y. Hamam & G. Attiya. Paris, France.

Roche, R., Lamanna, R., Delgado, M., Rocaries, F., Hamam, Y., Pecker, F. (2009). *Simulation of a cardiac cell. Parte I: An electro-chemical model. Accepted for publication to "Revista de la Facultad de Ingeniería de la Universidad Central de Venezuela"*. Caracas.

Sanchez, J., Garcia, M., Sharma, V., Young, K., Matlib, M., Sheu, S. (2001). Mitochondria regulate inactivation of L-type Ca^{2+} channels in rat heart. Journal of Physiology. Vol. 536.2, pp. 387-396.

Shampine, L. & Reichelt, M. (1977). The MATLAB ODE Suite. SIAM J. Scient. Comput., Vol. 18; pp. 1-22.

Sitsapesan, R. (1998). Regulation of ryanodine receptor channel gating. In: "The Structure and Function of Ryanodine Receptors". Imperial College Press; pp. 47-74.

Smith, G. & Steele, D. (1998). Measurement of SR Ca2+ content in the presence of caffeine in permeabilised rat cardiac trabeculae. European Journal of Physiology. Vol. 437, pp. 139-148.

Song, G., Tang, M., Liu, C., Luo, H., Liang, H., Hu, X., Xi, J., Gao, L., Fleischmann, B., Hescheler, J. (2002). Developmental changes in functional expression β-adrenergic regulation of If in the heart of mouse embryo. Cell research. Vol. 12 (5-6), pp. 386-394.

Tang, Y., & Othmer, H. (1994). Model of Calcium Dynamics in Cardiac myocytes Based on the Kinetics of Ryanodine-Sensitive Calcium Channels. Biophys. J. , Vol. 67; pp. 2223-2235.

Tominaga, M., Horie, M., Sasayama, S., Okada, Y. (1995). Glibenclamide, an ATP-sensitive K+ Channel blocker, inhibits cardiac cAMP-activated Cl- conductance. Circulation Research. Vol. 77, pp. 417-423.

Vigne, P., Breittmayer, J., Frelin, C. (1992). Thapsigargin, a new inotropic agent, antagonizes action of endothelin-1 in rat atrial cells. American Journal of Physiology Heart Circulation Physiology. Vol. 263, pp. H1689-H1694.

Winslow, R. & Greenstein, J. (2002). Regulation of Action Potential Duration in a Ventricular Myocyte Model Incorporating Local-Control of JSR Ca^{2+} Release. [On line], Satellite Symposium of the Japanese BME Society http://www.cmbl.jhu.edu.

Wu, Y., Colbran, R., Anderson, M. (2001). Calmodulin kinase is a molecular switch for cardiac excitation-contraction coupling. Proceeding of Natural Academy of Sciences. Of the United States of America. Vol. 98, No. 5, pp. 2877-2881.

Zhang, W. & Wong, W. (1998). Suppression of cAMP by phosphoinositol/Ca^{2+} pathway in the cardiac κ-opioid receptor. Cellular Physiology. Vol. 43, pp. C82-C87.

Zhang, X., Yuk-Chow, N., Russell, L., Musch, T., Cheung, J. (1999). In situ SR function in postinfarction myocytes. Journal of Applied Physiology. Vol. 87, Nº 6, pp. 2143-2150.

NOMENCLATURE

$\Delta_{calcium}$: Maximum calcium gradient.

$\hat{\Delta}_{calcium}$: Maximum calcium gradient estimated by the model.

η : Correction factor for the Na^{+}-Ca^{2+} exchanger current.

$\Re$: Ideal gas constant.

τ_d : L-channel kinetic constant.

$\sum rG(V, Ca_i^{2+}, k_i)_i$: Sum of generation rate of Ca^{2+} by chemical reactions.

$\sum rR(V, Ca_i^{2+}, k_i)_i$: Sum of removal rate of Ca^{2+} by chemical reactions.

a: Period of input voltage pulse.

A_{transf} : Transfer area of (sarcolemma or sarcoplasmic reticulum) membrane.

C : Cell membrane capacitance.

Ca_0^{2+}: Extra-cellular calcium concentration.

Ca_i^{2+}: Cytosol calcium concentration.

Ca_{SR}^{2+}: Sarcoplasmic reticulum calcium concentration.

CaM : Calcium-myofibril complex concentration.

C_{SC} : Specific membrance capacity.

C_{Ai}, C_{A0}: Concentration of component A inside and outside the membrane.

d : Fraction of active channels among the open L-channels.

d^{∞} : L-channel kinetic constant.

$D_{Ca^{2+}}$: Diffusion coefficient of calcium into the cytosol.

D_{AC} : Diffusion coefficient of component A into the cytosol.

E_{Ca} : Calcium equilibrium potential.

E_{K} : Potassium equilibrium potential.

E_{Ks} : I_{Ks} equilibrium potential.

E_{Na} : Sodium equilibrium potential.

f : Fraction of channels among the open L-channels inactivated by voltage.

f_{Ca} : Fraction of channels among the open L-channels inactivated by calcium.

f_{NaK} : Voltage-dependent Na^+-K^+ pump current factor.

F : Faraday constant.

FD_{LC} : Diffusive flow of calcium through the L-channels.

FD_{RC} : Diffusive flow of calcium through the R-channels.

$FQ_{ENa\text{-}Ca}$: Flow of calcium through the Na^+-Ca^{2+} exchanger.

FQ_{SERCA} : Flow of calcium through the SERCA pump.

$FQ_{Sarcolema}$: Flow of calcium through the Sarcolemma pump.

$\overline{G}_{Cab}$: Peak calcium background current conductance.

$\overline{G}_{K1}$: Peak inward rectifier potassium current conductance.

$\overline{G}_{Kp}$: Peak plateau potassium current conductance.

$\overline{G}_{Kr}$: Peak rapid component of the delayed rectifier potassium current conductance.

$\overline{G}_{Ks}$: Peak slow component of the delayed rectifier potassium current conductance.

$\overline{G}_{Na}$: Peak sodium current conductance.

$\overline{G}_{Nab}$: Peak sodium background current conductance.

$\overline{G}_{to}$: Peak transient outward potassium current conductance.

h : Fraction of channels among the open sodium channels rapidly inactivated by voltage.

I_{Ca} : L calcium channels current.

$\overline{I}_{Ca}$: Maximum L calcium channels current.

I_{Cab} : Calcium background current.

I_{Cahalf} : L calcium channels current level that reduces $\overline{P}_{CaK}$ by one-half.

I_{CaK} : Potassium current through the L calcium channels.

$I_{calcium}$: Calcium current.

$I_{ionicpumps}$: Ionic pumps currents.

I_{K1} : Inward rectifier potassium current.

I_{Kp} : Plateau potassium current.

I_{Kr} : Rapid component of the delayed rectifier potassium current.

I_{Ks} : Slow component of the delayed rectifier potassium current.

I_{Na} : Sodium channels current.

I_{Nab} : Sodium background current.

I_{NaCa} : Na^+-Ca^{2+} exchange current.

I_{NaK} : Na^+-K^+ pump current.

$\overline{I}_{NaK}$: Maximum Na^+-K^+ pump current.

I_{pCa} : Sarcolemma Ca^{2+} pump current.

$\overline{I}_{pCa}$: Maximum sarcolemmal calcium pump current.

$I_{potassium}$: Potassium current.

I_{sodium} : Sodium current.

I_{stim} : Stimulus current that triggers the membrane potential (square wave pulse).

I_{to} : Transient outward potassium current.

j : Fraction of channels among the open sodium channels slowly inactivated by voltage.

J_A : Diffusive flow of substance A.

k_{d1}, k_{d2} :Myofibril reaction kinetic constants.

k_i : Constants of kinetic reactions.

k_{NaCa} : Scaling factor for Na^+-Ca^{2+} exchanger current.

k_{sat} : Saturation factor for Na^+-Ca^{2+} exchanger current.

K : Na^+-Ca^{2+} exchanger maximum rate.

K_0^+ : Extra-cellular potassium concentration.

K_1^{∞} : Fraction of channels among the open potassium channels responsible of inward rectifier potassium current (I_{K1}).

K_i^+ : Intra-cellular potassium concentration.

K_{Kp} : Fraction of channels among the open potassium channels responsible of plateau potassium current (I_{Kp}).

K_m : Calcium half-saturation constant for Na^+-Ca^{2+} exchanger.

K_{mKo} : Potassium half-saturation constant for Na^+-K^+ pump current.

K_{mNa} : Sodium half-saturation constant for Na^+-Ca^{2+} exchanger current.

K_{mNai} : Sodium half-saturation constant for Na^+-K^+ pump current.

K_{mCa} : Calcium half-saturation constant for Na^+-Ca^{2+}exchanger current.

K_{mpCa} : Half-saturation constant for sarcolemma calcium pump current.

K_R : Fraction of channels among the open potassium channels instantly activated by voltage and responsible of rapid component of the delayed rectifier potassium current (I_{Kr}).

$K_{X_{Kr}}$: Fraction of channels among the open potassium channels quickly activated by voltage and responsible of rapid component of the delayed rectifier potassium current (I_{Kr}).

$K_{X_{Ks}}$: Fraction of channels among the open potassium channels slowly inhibited by voltage and responsible of slow component of the delayed rectifier potassium current (I_{Ks}).

$K_{X_{to}}$: Fraction of channels among the open potassium channels quickly activated by voltage and responsible of transient outward potassium current (I_{to}).

$K_{Y_{to}}$: Fraction of channels among the open potassium channels slowly inhibited by voltage and responsible of transient outward potassium current (I_{to}).

l : cell membrane wide.

l_1, l_{-1}, l_2, l_{-2} : Ryanodine-channels kinetic reactions constants (TANG and OTHMER, 1994).

m : Fraction of active channels among the open sodium channels.

M : Myofibrils concentration.

n : Saturation coefficient for Na^+-Ca^{2+} exchanger (n = 1).

Na_0^+ : Extra-cellular sodium concentration.

Na_i^+ : Intra-cellular sodium concentration.

p_1: SERCA pump maximum rate.

p_2 : Threshold SERCA pump concentration.

P : Fraction of open channels.

P_{Ca} : L calcium channels permeability to Ca^{2+}.

$\overline{P}_{CaK}$: L calcium channels permeability to K^+.

q_1: Sarcolemma pump maximum rate.

q_2 : Threshold sarcolemma pump concentration.

rG_{Miof} : Sum of generation rate of Ca^{2+} by myofibrils chemical reactions.

rR_{Miof} : Sum of removal rate of Ca^{2+} by myofibrils chemical reactions.

R_T : Ryanodine channels total concentration.

t : Time.

$t_{voltage}$: Duration of voltage cycle.

$\hat{t}_{voltage}$: Duration of voltage cycle estimated by the model.

$t_{calcium}$: Duration of calcium cycle.

$\hat{t}_{calcium}$: Duration of calcium cycle estimated by the model.

$t_{exctcalcium}$: Duration of excitation stage in calcium cycle.

$\hat{t}_{exctcalcium}$: Duration of excitation stage in calcium cycle estimated by the model.

$t_{relaxcalcium}$: Duration of relaxation stage in calcium cycle.

$\hat{t}_{relaxcalcium}$: Duration of relaxation stage in calcium cycle estimated by the model.

T : Temperature.

V : Voltage.

V_{cyt} : Cytosol volume.

V_{max} : Maximum voltage modulating the Na^{+}-Ca^{2+} exchanger kinetic reaction rate

V_{SR} : Sarcoplasmic reticulum volume.

x_1: Fraction of Ryanodine channels in the transition state *R*.

x_2: Fraction of Ryanodine channels in the transition state RC^{+} (open channel).

x_3: Fraction of Ryanodine channels in the transition state $RC^{+}C^{-}$.

x_4: Fraction of Ryanodine channels in the transition state RC^{-}.